ISSN 1392 - 1207. MECHANIKA. 2008. Nr.6(74)

Investigation of three-dimensional granular stresses in pyramidal container after filling

R. Balevičius*, R. Kačianauskas, V. Vadluga*****

**Vilnius Gediminas Technical University, Saulėtekio 11, 10223 Vilnius, Lithuania, E-mail: Robertas.Balevicius@st.vgtu.lt*

***Vilnius Gediminas Technical University, Saulėtekio 11, 10223 Vilnius, Lithuania, E-mail: rkac@fm.vgtu.lt*

****Vilnius Gediminas Technical University, Saulėtekio 11, 10223 Vilnius-40, Lithuania, E-mail: vvad@fm.vgtu.lt*

1. Introduction

Various attempts have been made to produce design models defining the wall pressure occurring after filling of the granules into containers. In general, this pressure is resulted from the stresses developed within granular material, which, in the case of pyramidal container, are distributed over three dimensions. The investigation of the above stress and resulting pressures are important factor in design of industrial operations. A comprehensive review on the foundations of granular flow and designed methodologies, presented from the engineering point of view, is given by Roberts [1].

Many advances of granular theory and industrial application have been achieved through the continuum-based models. The method of the differential slices introduced by Janssen [2] and extended by Walker [3] along with a set of correction factors is often used for design purposes [4, 5]. However, these extensions with a priori assumed stress distribution within granular material are mainly attributed to the plane strain hoppers and cannot directly be applied to 3D wedge-shaped hopper.

The stress patterns have a major influence on the magnitude of wall pressure, and the way of eliminating assumptions about the stress distribution within container has been usually associated with the application of the method of characteristic or FEM for solving the differential equations of continuum mechanics [6-9]. The evaluation of the state of art in the implementation of the FEM technique was made by Holst *et. al.* [10]. They showed the strengths and weaknesses of FEM in modelling silo filling processes.

Various classical (relying on the linear elastic Hooke's law as well as perfectly plastic relations with various yield conditions and the associated or non-associated flow rules) and nonclassical (based on the assumption of density hardening) models and theories were elaborated within this category [11, 12]. The analytical models for evaluating filling and discharge state of the elastic and elastic-plastic material were proposed by Mróz and Sielamowicz [13], Drescher [14].

However, the continuum-based methods have serious difficulties in capturing the discrete nature of granular material. Thus, granular material may be represented as discontinuous media by using discrete element method (DEM) [15], as an alternative.

Campbell and Brennen [16], Walton [17] and Thornton [18] were the first to apply discrete methods to silo flow problems. In their approach, a limited number of particles was used and, in spite of this fact, some interesting results concerning the flow rate and velocity profiles were obtained. These simulations were continued in the work by Kafui and Thornton [19].

It should be noted, that the data on numerical analysis of stresses by applying DEM is rather scarce, see Landry et al. [20], Zhu and Yu [21], Balevičius et. al. [22], while the any numerical studies of three-dimensional stress fields within pyramidal container have not been found.

The current research addresses three-dimensional granular stress analysis in pyramidal container after the filling. The particular manifest is to modify and investigate the stress distribution factor employed in differential slice method for a three-dimensional case.

2. Modelling approach

The experimental investigations of stress, acting within the granular material, are complicated, requiring noninvasive and scrupulous contact force measurements [23, 24]. An alternative is to find the particle contact forces basing on contact mechanics relationships and then average these forces and their contact locations over the particular volumes. Such numerical analysis links the microscopic variables in the discrete concept to the macroscopic variables in the continuum approach

Thus, the microscopic stresses in granular material are characterized by stress tensor. Tensor components σ_{ij} are obtained from the microscopic quantities by applying homogenization over the given volume V of the particle assembly [25]

$$\sigma_{ij} = \frac{1}{V}\sum_{c\in V} F_i^c l_j^c \text{ , } i, j = 1, 2, 3, \tag{1}$$

where F^c and l^c are vector of the contact forces and the contact positions, while c stands for a set of inter-particle contacts. Subscripts $i(j)$ denotes directions of Cartesian components of the above vectors and stress tensor, thus, $i, j = x, y, z$.

In general, the symmetrical stress tensor σ_{ij} defines the three-dimensional state of stresses which act on three mutual perpendicular planes at a given point of granular matter.

Evaluating basic vectors of the contact consider the kinematics and contact geometry of two spherical particles plotted in Fig. 1.

Two particles in contact, i and j, are defined by their positions $\mathbf{x}_i$ and $\mathbf{x}_j$, representing the locations of the centres of gravity O_i and O_j (Fig. 1). The position of parti-

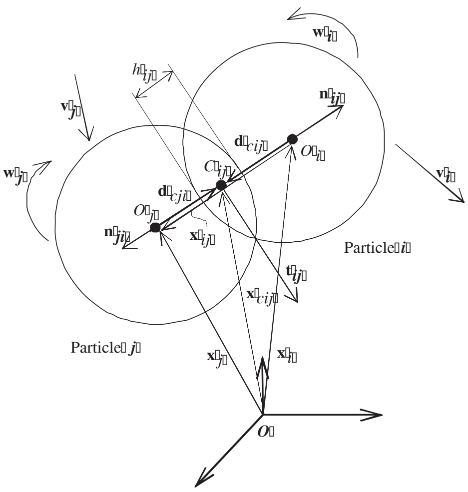

Fig. 1 Outline of the particles' contact geometry

cles is time-dependent. The particles are subjected to the translational velocities $\mathbf{v}_i$ and $\mathbf{v}_j$, as well as the rotation velocities $\mathbf{w}_i$ and $\mathbf{w}_j$.

Employ the DEM approach to find contact forces acting within granular media. In terms of DEM, the particles are treated as individual objects with their own dynamical parameters (position, velocity, etc.). Therefore, the dynamics of each particle can be defined by forces and torques acting on the particle and described by a system of dynamical equations within Newton's law

$$m_i \frac{d^2 \boldsymbol{x}_i}{dt^2} = \sum_{j=1, j\neq i} \boldsymbol{F}_{ij} + m_i \boldsymbol{g} \qquad (2)$$

$$I_i \frac{d^2 \boldsymbol{\theta}_i}{dt^2} = \sum_{j=1, j\neq i} \boldsymbol{d}_{cij} \times \boldsymbol{F}_{ij} \qquad (3)$$

where $\boldsymbol{x}_i$, $\boldsymbol{\theta}_i$ are the vectors of the position of the centre of gravity and the orientation of the particle (Fig. 1), m_i is the mass of the particle i ($i = 1, N$), I_i is the inertia moment of the particle, $\boldsymbol{g}$ is the vector of gravity acceleration, while t is the time considered.

In general, for three-dimensional grains with arbitrary shapes, however, the inertia moment I must be calculated in every time step according to the new orientation of the particle. Therefore, two coordinate systems, namely, local coordinate system, and a moving Cartesian coordinate system which is fixed with the particle and whose axes are the principal axes of inertia are usually considered in modelling of the non-spherical grains. Thus, the diagonal inertia tensor $I_i = (I_{1i}, I_{2i}, I_{3i})$ in a body-fixed, i.e., local coordinate system, is used instead of its scalar. For spherical particles, we get $I_{1i} = I_{2i} = I_{3i} = I_i$, and local coordinate system becomes the same as the global one. Therefore, equation for rotational motion of the particle is rewritten in a simpler form using (3).

The contact deformation of the particle i with respect to another particle j is approximated by a representative overlap area in the vicinity of the contact centre point C_{ij}. This allows the implementing of the contact force models based on a single particle contact mechanics.

Generally, the forces, as the right-hand terms in Eqs. (2) and (3), depend on the particle geometry and mechanical properties as well as on the constitutive model of the particle interaction. The presented inter-particle contact model considers Hooke's law of spring interaction, static and dynamic frictions as well as nonconservative viscous damping forces given explicitly in [26, 28].

Referring back to Eqs. (2) and (3) it is necessary to explain, that vector $\boldsymbol{F}_{ij}$ represents the inter-particle or particle-wall contact forces acting on the contact centre point C_{ij}, while $\boldsymbol{d}_{cij}$ is the vector specifying the position of the contact point C_{ij} with respect to the centers of the contacting particles.

Now, it could be shown, that components of the vectors $\boldsymbol{F}^c$ and $\boldsymbol{l}^c$ used for evaluation of the stresses are composed of components of the above vectors $\boldsymbol{F}_{ij}$ and $\boldsymbol{d}_{cij}$ (Fig. 1). Actually, evaluation of the stresses σ_{ij} has to be presented in a form of time histories $\sigma_{ij}(t)$ tracked until the end of filling period.

Numerical implementation of formula (1) into DEM-based analysis and the obtained results verification was given in [29]. Meanwhile, the DEM technique used was described in detail in [26], [30]. Its implementation to the analysis of the filling processes in hoppers was also discussed in [22], [31].

3. Problem description

Granular material is modeled as an assembly of noncohesive spherical $N = 1980$ particles. The particle

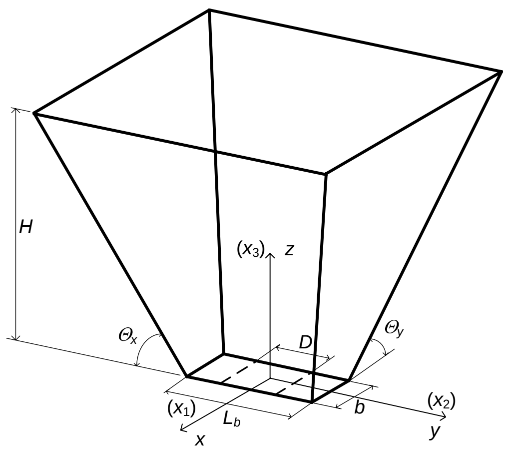

a

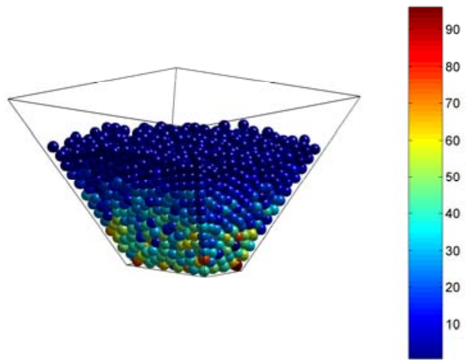

b

Fig. 2 Geometry of the container (a) and particles with contact forces obtained at the end of filling of container (b) radii R_i varying over the range of 0.03 and 0.035 m were generated with an uniform distribution. Total mass M of the material was equal to $M = 143.7$ kg. Elasticity modulus of the particle was equal to $E = 0.3{\cdot}10^6$ Pa. Viscous damping is described by coefficients $\gamma_n = 60$ s^{-1} and $\gamma_t = 10$ s^{-1} which are defined in normal and tangential contact directions. Inter-particle and particle-wall friction is characterized by friction coefficient, $\mu = 0.3$.

The characteristic dimensions of the outlet are traditionally related to the maximal diameter d of the particle as $D = 8.6d$ and $b = 4.3d$; while the container's height and width are coupled with acute angles $\theta_y = 68°$, $\theta_x = 62°$ providing for $H = 2.88D$. The geometry of the converging pyramidal container is plotted in Fig. 2, a. Walls (including the bottom) are assumed to be rigid and considered as the fixed boundaries having friction. The state of granular assembly after the filling is plotted in Fig. 2, b. The color scale indicates the magnitude of the particle contact forces defined in N.

4. Numerical results

Normal stresses σ_{ii} (where $I = 1, 2, 3$) obtained by formula (1) and relying on the particles forces data shown in Fig. 2, b are plotted in Fig. 3. The stresses are given in Pa there.

As can be seen from these plots, the distribution of the normal stresses has a convex shape with peak values at the centre and lower values at the wall planes. The decrease in stresses going from centre of the hopper to its wall occurs due to shear stresses originated from particles friction. The obtained convex shape of σ_{33} is well-coincident with the asymptotic stress distribution found by Drescher [14] by using the method of characteristics. It is obvious that horizontal stress variation is the function of the coordinates x and y, see Fig. 3. It is known, however, that an erroneous assumption about the constant horizontal stresses variation was used by Walker [3]. In addition, a condition $|\sigma_{33}| > |\sigma_{22}| > |\sigma_{11}|$ is satisfied, suggesting that the active stress state occurs within the entire container after the filling is completed.

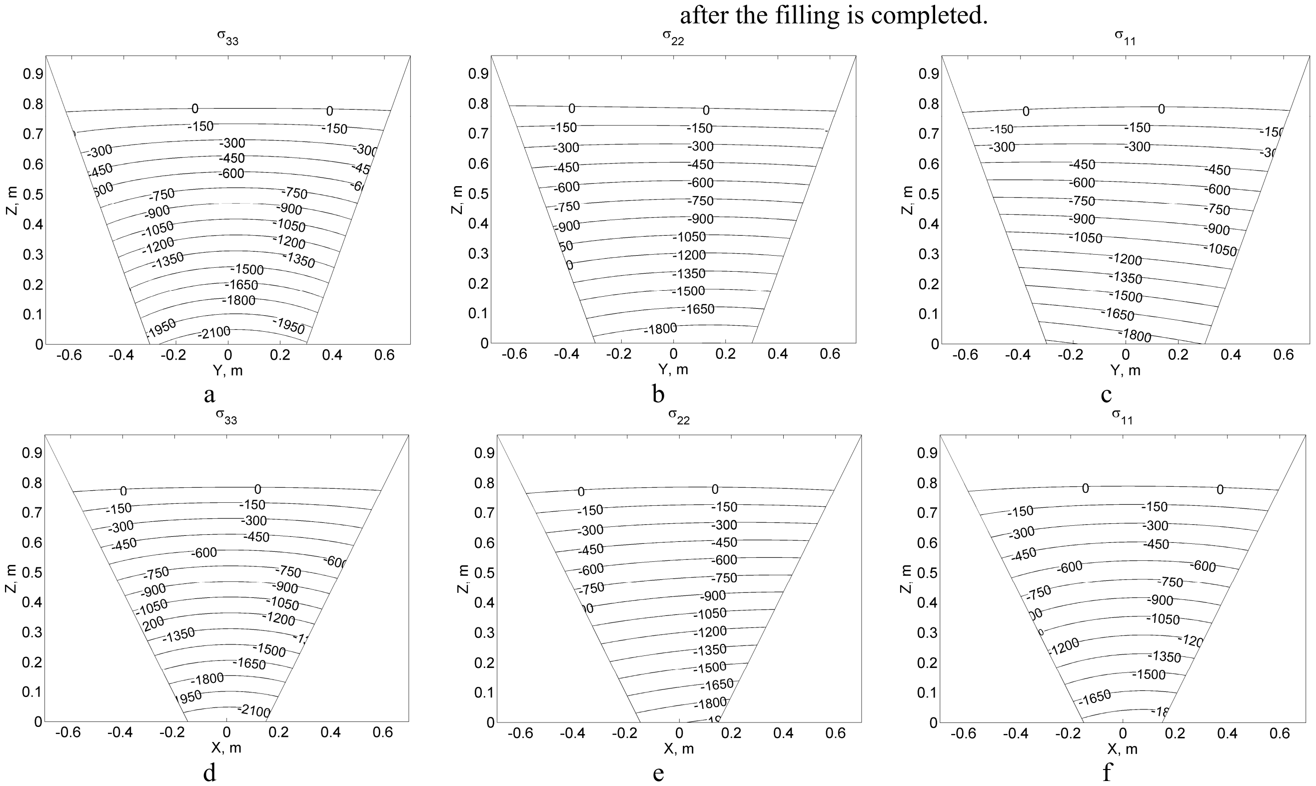

Fig. 3 Distribution of normal stresses in two perpendicular mid-planes at the end of filling, (a-c) plane Oyz, (d-f) plane Oxz

Finally, it should be noted that discrete particle micromechanical properties contribute stress fields that would be more precise with increasing the number of particles in the model.

5. Discussion

The character of the obtained stresses presented in the previous section shows that DEM model used with relationship (1) is able to represent the stress fields of granular continuum within pyramidal container. Thus, on the basis of the above results a modification in a frame of the method of differential slices [4] can be now considered.

Generally, the method of differential slices employs force balance on the horizontal infinitesimal slice bounded by the container walls. The existing models are characterised by explicit relations among stress components tailored for specific geometries. In particular, it takes the stress components as related by the various yield conditions. An important issue is how to relate the distribution of stresses occurring within granular material with the wall pressure.

In general, any distribution of stresses over the finite dimension of arbitrary differential slice with coordinate z measured vertically from the apex of the container can be postulated in order to find the corresponding average stresses. Therefore, the average stresses acting on differential slice is simply represented as an uniformly distributed. Meanwhile, the evaluation of normal stresses decreasing towards the walls (due to contribution of shear stress) may be expressed adopting the stress distribution factor *D* introduced by Walker [3]. Originally, this factor was proposed for the case of plane hopper. In particular, by referring to stress σ_{33} in the section $x = 0$, the factor D_{33} expresses the ratio of actual stresses on the walls $\sigma_{33}(0, y_w, z)$ to mean granular stresses $\langle\sigma_{33}(0, y, z)\rangle$.

Based on the determined spatial stress variation within granular material we arrived at the following expression for the distribution factor of normal stress components σ_{ii} ($i = 1, 2, 3$) for the case of the three-dimensional container. In pyramidal container, the hopper geometry dependent factor *D* will be different for two perpendicular walls denoted hereafter by subscripts *wx* and *wy,* respectively

$$D_{ii\,\mathrm{w}x}(z) = \frac{\langle\sigma_{ii\,\mathrm{w}x}(z)\rangle}{\langle\sigma_{ii}(z)\rangle} \tag{4}$$

$$D_{ii\,\mathrm{w}y}(z) = \frac{\langle\sigma_{ii\,\mathrm{w}y}(z)\rangle}{\langle\sigma_{ii}(z)\rangle} \tag{5}$$

where $\langle\sigma_{ii\,\mathrm{wx}}(z)\rangle = \langle\sigma_{ii}(x_w, 0, z)\rangle$, $\langle\sigma_{ii\,\mathrm{wy}}(z)\rangle = \langle\sigma_{ii}(0, y_w, z)\rangle$ and $\langle\sigma_{ii}(z)\rangle = \langle\sigma_{ii}(x, y, z)\rangle$ are the mean normal stresses at the walls and the average stresses acting in the slice.

Homogenization of Eqs. (4) and (5) may be performed by integrating over slice area *A*(*z*) or lengths of the slice $L_x(z)$ and $L_y(z)$ on the corresponding container wall, respectively. Finally, taking into account the definitions of container geometry (Fig. 2, a) we get the following formulae

$$D_{ii\,wx}(z) = \frac{2z\cot(\theta_x)\int_{L_y(z)}\sigma_{ii}\,(x_w, y, z)\,dy}{\iint_{A(z)}\sigma_{ii}\,(x, y, z)\,dxdy} \tag{6}$$

$$D_{ii\,wy}(z) = \frac{2z\cot(\theta_y)\int_{L_x(z)}\sigma_{ii}\,(x, y_w, z)\,dx}{\iint_{A(z)}\sigma_{ii}\,(x, y, z)\,dxdy} \tag{7}$$

To illustrate the averaging methodology and the influence of three-dimensionality of the distribution, variation of σ_{33} over the slice located at the height of 0.5 m from the bottom is plotted in Fig. 4, a. An approximation of integrals in Eqs. (6) and (7) was computed numerically via the trapezoidal method.

Here, the convex surface shows actual variation of $\sigma_{33}(x, y, z)$, while the horizontal plane represents the average stress value $\langle\sigma_{33}(x, y, z)\rangle$. The line above this plane stands for the mean stress $\langle\sigma_{33}(0, y, z)\rangle$ averaged only along *y* axis, for coordinate $x = 0$, which is considered in two-dimensional models by neglecting variation of stresses in perpendicular direction. The lower line represents the mean stresses $\langle\sigma_{33\,wy}(x, y_w, z)\rangle$ on the wall perpendicular to plane Oyz.

The graphs illustrating variation of the distribution factor of the vertical stresses $D_{33\,\mathrm{wy}}(z)$ over the height for the container considered are plotted in Fig. 4, b. The first curve represents Walker's distribution factor derived for the plane case, while the second curve reflects factor $D_{ii\,\mathrm{wy}}(z)$ obtained by the proposed relations (6) and (7). In particular, the difference between both factors is significant in the upper layers of the material, indicating three-dimensional stress contribution which would be of major importance in the analysis of pyramidal container. In addition, the convergence tendency of both curves can be observed with the increasing material depth, while their values ranging between 0.9 and 1.0 are quite typical for the active stress state [4]. The third curve presenting the relationship between $\langle\sigma_{33}(x, y, z)\rangle$ and $\langle\sigma_{33}(0, y, z)\rangle$ evaluates a decrease of stress in pyramidal container caused by the

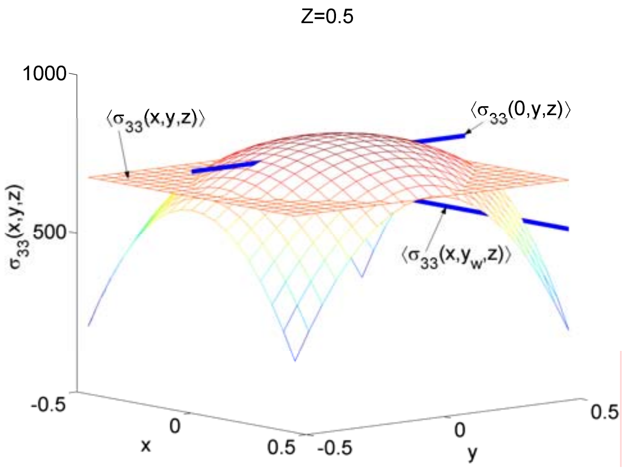

a

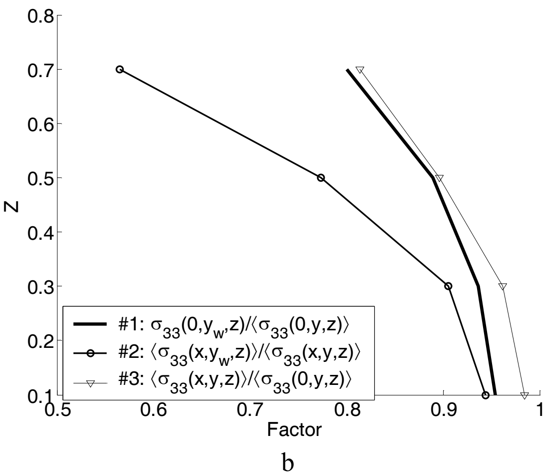

b

Fig. 4 Illustration of cutaway of the obtained vertical stresses $|\sigma_{33}|$ at the height of 0.5 m (a); stress distribution factors (b)

out-of-plane stress component. It can be seen that three-dimensional stress contribution decreases along with decrease of cross-section of the container. In addition, the peak of stress acting on the walls is located at the centre of wall (Fig. 4, a), while near the corners the stress reduces due to shear.

6. Concluding remarks

The 3D variation of stress fields occurring in granular material after the filling of pyramidal rectangular container were investigated by applying the DEM. In particular, the influence of the three-dimensional variation of the stress was examined within the framework of differential slice method.

On the basis of the obtained results the following conclusions have been drawn:

1. Generally, neglecting of three-dimensional variation of stresses yields overestimated values of the mean stress and stress distribution factor. This tendency may be of the primary importance for the discharge process, where the granular material is undergone passive stress regime.

2. The above illustrated difference should be taken into account by considering the equilibrium of differential slice in pyramidal container. In addition, performing the design, the stress acting on pyramidal container wall must be calculated at its center, where granular material stress has the maximal value, while near the corners this stress reduces.

3. Despite a small number of particles used the obtained results are quite representative and qualitatively comparable with the continuum-based predictions, while the discrete element method could be used in the future for revising continuum-based models and three-dimensional problems, in particular. The refined 3D DEM models, including discharge flow, are under development now.

References

1. **Roberts, A.W.** Particle and bulk solids handling technology – bridging the theory practice gap. -Fifth World Congress on Particle Technology, 2006, Orlando, Florida, USA, CD ROM proceedings, p.1-38.
2. **Janssen, H.A.** Versuche über Getreidedruck in Silozellen. -Z. Ver. Dtsch. Ing., 1895, v.39, No35, p.1045-1049 (in German).
3. **Walker, D.M**. An approximate theory for pressures and arching in containers. -Chemical Engineering Science, 1966, v.21, No8, p.975-997.
4. **Nedderman, R.M.** Statics and Kinematics of Granular Materials. -New York: Cambridge University Press, 1992.-352p.
5. **Schwedes, J., Feise, H.** Modelling of pressures and flow in silos. -Chemical Engineering & Technology, 1995, v.18, p.96-109.
6. **Horne, R.M., Nedderman, R.M.** Analysis of the stress distribution in two-dimensional bins by the method of characteristics. -Powder Technology, 1976, v.14, p.93-102.
7. **Wu, Y-H. Collinson, R.** Determination of velocity and stress discontinuities in quasi-static granular flows. -Anziam Journal, 2000, v.42, NoE, p.C1558-C1579.
8. **Tejchman, J., Klisinski, M.** FE-studies on rapid flow of bulk solids in silos. -Granular Matter, 2000, v.3, p.215-229.
9. **Guaita, M., Couto, A. Ayuga, F.** Numerical simulation of wall pressure during discharge of granular material from cylindrical silos with eccentric hoppers. -Biosystems Engineering, 2003, v.85, No1, p.101-109.
10. **Holst, J.M.F.G., Ooi, J.Y., Rotter, J.M., Rong, G.H.** Numerical modeling of silo filling: I. Continuum analyses. -J. of Engineering Mechanics, 1999, v.125, No1, p.94-103.
11. **Spencer, A.J.M., Hill, J.M.** Nondilatant double-shearing theory applied to granular funnel-flow in hoppers. -J. of Engineering Mathematics, 2001, v.41, p.55-73.
12. **Bräuer, K., Pfitzner, M., Krimer, D.O., Mayer, M., Jiang, Y., Liu, M.** Granular elasticity: stress distributions in silos and under point loads. -Physical review E, 2006, v.74, p.061311-1 – 061311-10.
13. **Mróz, Z., Sielamovicz, I.** Deformation zones in granular materials in converging hoppers during filling and emptying processes. -Engineering Transactions, 2003, v.51, No4, p.461-491.
14. **Drescher, A.** Analytical Methods in Bin-Load Analysis. -New York: Elsevier, 1991.-255p.
15. **Cundall, P.A., Strack, O.D.L.** A discrete numerical model for granular assemblies. -Geotechnique, 1979, v.29, No1, p.47-65.
16. **Campbell, C.S. Brennen, C.E.** Computer simulation of shear flows of granular material. -J. of Fluid Mechanics, 1985, v.151, p.167-188.
17. **Walton, O.R.** Particle –dynamic calculations of shear flow. -Mechanics of Granular Materials: New Models and Constitutive Relations, 1983, p.327-338.
18. **Thornton, C.** Application of DEM to process engineering problems. -1st US Conference on Discrete Element Methods, Colorado School of Mines Press, 1989, p.87-100.
19. **Kafui, K.D. Thornton, C**. Some observations on granular flow in hoppers and silos. -Powders & Grains 97, 1997, p.511-514.
20. **Landry, J.W., Grest, G.S., Plimpton, S.J.** Discrete element simulations of stress distributions in silos: crossover from two to three dimensions. -Powder Technology, 2003, v.139, p.233-239.
21. **Zhu, H.P., Yu, A.B.** Steady-state granular flow in a 3D cylindrical container with flat bottom: macroscopic analysis. -Granular Matter, 2005, v.7, p.97-107.
22. **Balevičius, R., Kačianauskas, R., Mroz, Z., Sielamovicz, I.** Discrete particle investigation of friction effect in filling and unsteady/steady discharge in three-dimensional wedge-shaped hopper. -Powder Technology, in press.
23. **Howell, D.W., Behringer, R.P., Veje, C.T.** Fluctuations in granular media. -Chaos, 1999, v.9, No3, p.559-572.
24. **Drescher, A., de Josselin de Jong, G.** Photo-elastic verification of a mechanical model for the flow of granular material. -J. Mech. Phys. Solids, 1972, v.20, No5, p.337-351.
25. **Christoffersen, J., Mehrabadi, M., Nemat-Nasser, S.** A micro-mechanical description of granular material behavior. -J. Appl. Mech., 1981, v.48, No2, p.339-344.
26. **Balevičius, R., Džiugys, A., Kačianauskas, R.** Discrete element method and its application to the analysis of penetration into granular media. -J. of Civil Engineering and Management, 2004, v.10, No1, p.3-14.
27. **Džiugys A., Navakas R., Šlančiauskas A., Stravinskas G., Kačianauskas R.** Numerical simulation of mixing and segregation of granular material. -Mechanika. -Kaunas: Technologija, 2005, v.53, No3, p.52-56.
28. **Džiugys, A., Peters, B.J.** An approach to simulate the motion of spherical and non-spherical fuel particles in combustion chambers. -Granular Material, 2001, v.3,

No4, p.231-266.
29. **Balevičius, R., Markauskas, D.** Numerical stress analysis of granular material. -Mechanika. -Kaunas: Technologija, 2007, Nr.4(66), p.12-17.
30. **Balevičius, R., Kačianauskas, R., Džiugys, A., Maknickas, A., Vislavičius, K.** Investigation of performance of programming approaches and languages used for numerical simulation of granular material by the discrete element method. -Computer Physics Communications, 2006, v.175, No6, p.404-415.
31. **Balevičius, R., Kačianauskas, R., Mroz, Z., Sielamowicz, I.** Microscopic and macroscopic analysis of granular material behaviour in 3D flat-bottomed hopper by the discrete element method. -Archives of Mechanics, 2007, v.59, No3, p.231-257.

R. Balevičius, R. Kačianauskas, V. Vadluga

TRIMATIS GRANULIUOTOS MEDŽIAGOS ĮTEMPIŲ, ATSIRADUSIŲ PIRAMIDINĖJE TALPYKLOJE PO SUPYLIMO, MODELIAVIMAS

R e z i u m ė

Straipsnyje pateikiamas trimatis granuliuotos medžiagos įtempių, veikiančių piramidinėje talpykloje po medžiagos supylimo, modeliavimas. Erdviniai įtempių laukai apskaičiuoti nustačius daleles veikiančias kontakto jėgas ir jas suvidurkinus užsiduotame medžiagos tūryje. Įtempių pasiskirstymo laukai patvirtinti remiantis žinomais kontinuumo mechanikos teiginiais. Įtempių pasiskirstymo koeficientas, naudojamas diferencialinio pjūvio metodikoje, patikslintas atsižvelgiant į nustatytus įtempių erdvinio būvio rezultatus.

R. Balevičius, R. Kačianauskas, V. Vadluga

INVESTIGATION OF THREE-DIMENSIONAL GRANULAR STRESSES IN PYRAMIDAL CONTAINER AFTER FILLING

S u m m a r y

The discrete element simulation was performed to evaluate granular stresses in pyramidal container after the filling. The 3D stress fields were obtained on the basis of a micromechanical approach by calculating inter-particle contact forces and their subsequent homogenization in the given volume of material. Stress distributions were confirmed the continuum-based indications. According to the results obtained, the stress distribution factor was corrected relying on the influence of three-dimensionality in the frame of the differential slice approach.

Р. Балявичюс, Р. Качанаускас, В. Вадлуга

ТРЕХМЕРНЫЙ АНАЛИЗ НАПРЯЖЕНИЙ ГРАНУЛИРОВАННОГО МАТЕРИАЛА В ПИРАМИДНОМ КОНТЕЙНЕРЕ ПОСЛЕ ЗАПОЛНЕНИЯ

Р е з ю м е

На основе метода дискретных элементов проведен анализ учета напряжений, действующих в гранулированном материале после заполнения пирамидного контейнера. Трехмерные поля распределения напряжений установлены на основе микромеханического подхода при учете сил, действующих непосредственно на частицы материала с их последующей гомогенизацией в заданном объеме материала. Распределение напряжений подтверждено их совместимостью с известными предпосылками механики сплошной среды. Полученные результаты использованы для учета влияния трехмерности на коэффициент распределения напряжений в методе дифференциального сечения.

Received August 18, 2008
Accepted October 09, 2008